euronoise

Modeling high-frequency reverberation and propagation loss in support of a submarine target strength trial

Boris Vasiliev and Art Collier

DRDC Atlantic, 9 Grove St., Dartmouth, NS, Canada B2Y 3Z7
boris.vasiliev@drdc-rddc.gc.ca

In November 1994, DRDC Atlantic measured target strength of a submarine at 20–40 kHz at a shallow site in the North West Atlantic. In the absence of direct propagation loss measurements, the measured reverberation was used to verify the environmental and sonar parameters for propagation loss predictions required for target strength data analysis. The site bottom was gravel and during the trial the surface wind speeds were 2–6 m/s. The assumed APL-UW interface models were a surface with negligible loss and scattering strength, and a bottom with low loss and high scattering strength. For ranges less than 1.8 km, the CW reverberation at 24, 28, and 39 kHz agreed with CASS-GRAB predictions; beyond 1.8 km, the model output underestimated the measurements. The LFM reverberation at 21, 28, and 36 kHz for 2 kHz bandwidth signals matched the CW reverberation after compensation for the pulse range resolution and frequency differences in the beam responses and volume attenuation. The propagation loss was estimated by fitting a power law dependence to the predicted losses in the submarine operating depth envelope. The estimated loss yielded range independent target estimates and was assumed representative of the propagation conditions during the trial.

1 Introduction

In November 1994, the DRDC Atlantic, together with UK and US research agencies, measured target strength of a Canadian Navy submarine. The trial took place over the La-Have Bank on the Nova Scotia's eastern coast, approximately 200 km south of Halifax, NS.

During the trial, propagation loss was not measured, but numerous measurements of reverberation from CW and LFM pulses were collected. In the absence of the propagation loss measurements, the reduction of the target echo intensity to target strength relied on the propagation loss predictions. The environmental and sonar parameters for the propagation loss modeling were verified by comparing the measured and modeled CW and FM reverberation. Similar analysis on data collected 20^{h} after the trial at the same site was already reported in [1, 2]; however, the findings were inconsistent with the bottom survey results and reverberation measured during the target strength trial, and additional review of the data was required.

This paper provides a short overview of the environmental modeling that supported the target strength data analysis. After review of the Seahorse sonar and environment, the CW reverberation measurements are compared with the CASS-GRAB, [3], predictions and FM reverberation measurements. The propagation loss modeling is described and an example of the estimated submarine target strength is presented.

2 Seahorse sonar

The Seahorse sonar is an experimental sonar developed at DRDC Atlantic in the mid-1990's, [4]. The sonar was deployed in a bottom-tethered configuration at 40–43 m depth. The sub-surface platform was connected to a surface buoy which was equipped with two radio systems linking the sonar to the support ship CFAV QUEST. The command link controlled sonar heading, tilt, source level, and transmitted waveforms; the second link relayed acoustic and non-acoustic data to the ship.

The sonar transmitted CW, LFM, or combination (CW followed by LFM) pulses. The CW pulses were 60 or 80 ms long with center frequencies 24, 28, and 39 kHz. The LFM pulses were 2 kHz wide, 160 ms long with center frequencies 21, 28, and 36 kHz. The ping repetition rate was 1 ping in 15 seconds. The 20–24 kHz and 35–39 kHz pulses were equalized for the transducer response and their source level was 202 ± 1 dB re 1 µPa @ 1 m. The 27–29 kHz pulses were unequalized for the transmitter response and their source level was 10 dB higher at 211 dB re 1 µPa @ 1 m. All pulses were shaded with Tukey-25% window to reduce spectral leakage. The receive sensitivity in the 20–40 kHz band was -179 ± 3 dB re V/µPa.

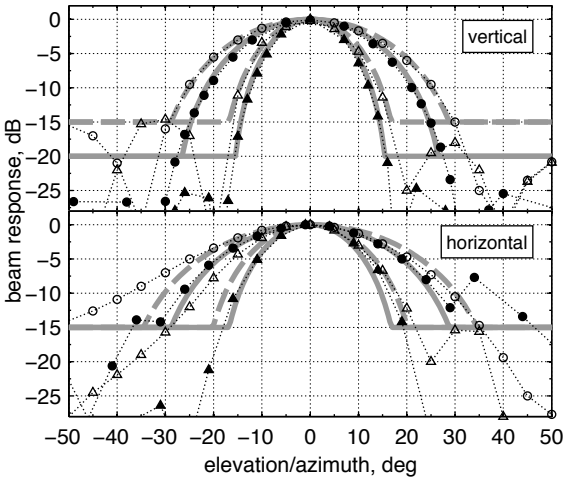

Fig. 1: Seahorse sonar vertical and horizontal beams. Measured beam responses: ···o·· 21 kHz receive, ···●·· 21 kHz transmit, ···▲·· 36 kHz receive, and ···▲·· 36 kHz transmit. Modeled beam responses: — — receive and ——— transmit.

The measured vertical and horizontal beam responses of the sonar at 21 and 36 kHz together with the parametric fits to the measurements are shown in Fig. 1. The parametric beam response was a main lobe with a fixed level, B_0, for sidelobes. The main lobe response was

$$B(\theta) = 10\log\left(\frac{\sin u}{u}\right)^2, \quad |\theta| \le \theta_{B_0} \tag{1}$$

where $u = 2\pi\theta(D/2)/\lambda$, θ is the elevation or azimuthal angle and λ is the acoustic wavelength. The characteristic size of the sonar transducer, D, determines the main lobe width for a given frequency. The transition from the main lobe to the sidelobes occurs at θ_{B_0} where the main lobe response first drops below the parametric sidelobe level. These levels were between -20 and -15 dB for horizontal and vertical beams.

The parametric beam responses were used in the acoustic modeling. The characteristic transducer sizes, estimated from the beam measurements, were 14 cm for vertical transmit, 12 cm for vertical receive, 12 cm for horizontal transmit, and 10 cm for horizontal receive. These parameters yielded good agreement between the parametric and measured beams

at 21 and 36 kHz as shown in Fig. 1. Beam patterns at other frequencies were interpolated via Eq.(1). The parametric −3 dB beam widths for transmit/receive/vertical/horizontal beams were 26–36° at 21 kHz and 14–20° at 39 kHz.

3 Environment

Bathymetry at the trial site was surveyed intermittently over several days prior to the trial. The survey was along north–south tracks 0.3–0.4 km apart with individual soundings spaced 50–100 m along each track. The depth contours for the site are shown in Fig. 2. The sharp corners in the contour lines were due to the sensitivity of the contours to the smoothing and griding schemes applied to reduce the variability in the depth measurements (2–4 m between consecutive samples). The contours indicate that bottom slope is small (the water depth decreased from 106 m to 102 m over 2 km) and for reverberation and propagation loss modeling the bottom depth was assumed constant at 104 m.

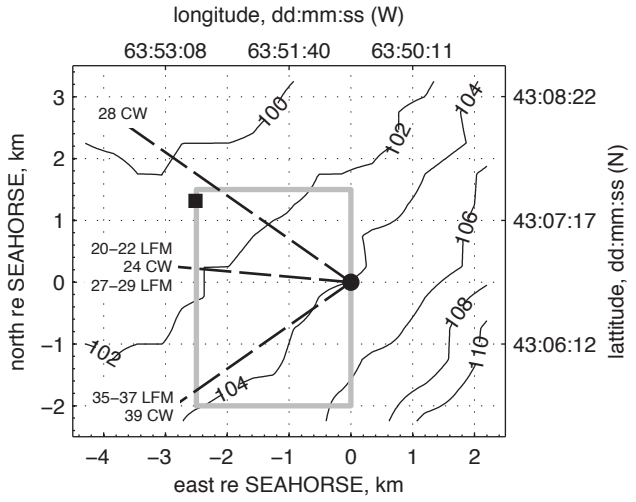

Fig. 2: Trial site bathymetry. Depth is in meters. Seahorse sonar position is ●. Bottom survey location is ■. ——— delimits trial site. — — are bearings for reverberation measurements; frequencies are in kHz.

The bottom composition at the trial site was surveyed in a separate experiment 8 months after the trial, [5]; the survey location is shown in Fig. 2. The survey indicated that the bottom was gravel and cobble with numerous highly reflective point scatters which were interpreted as boulders up to 3 m in diameter. No bottom penetration was observed in the sub-bottom profiler records suggesting a complete absence of soft sediments.

For the paths significant to reverberation and propagation loss the grazing angles were low. For these angles (5–20°) rough surface scattering dominates forward reflection loss and backscattering from hard bottoms such as that at the trial site. To account for rough surface scattering, the bottom reflection loss was assumed to be −1.5 dB/reflection, [6]. The APL-UW bottom scattering for gravel (grain size index −3) is shown in Fig. 3, [6]; for shallow angles, the scattering strength follows Lambert's rule, $ss_b \sim \sin^2\theta$, with proportionality coefficient −10 dB.

During the trial, the wind speed was low to moderate, increasing from 2 to 6 m/s. For the shallow grazing angles (5–20°) of the significant propagation paths, attenuation and

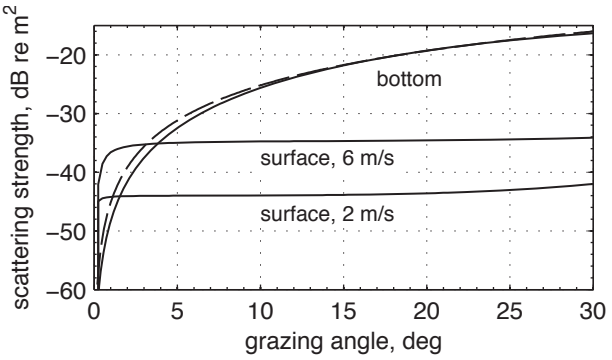

Fig. 3: APL-UW bottom and surface scattering strengths at 30 kHz. — — is Lambert's law with proportionality constant −10 dB.

scattering from sub-surface bubbles dominates forward reflection loss and backscattering from the surface. The typical threshold for appearance of bubbles is 3–6 m/s; below the threshold, in the absence of bubbles, the surface is a nearly lossless reflector of sound, [6]. The surface reflection loss was assumed 0 dB/reflection, consistent with the low wind speeds. The APL-UW surface scattering strength for 2 and 6 m/s is shown in Fig. 3.

Two sound speed profiles were measured: SSP1, 11 hours before the trial start, and SSP2, 4 hours after the trial end. The measured profiles are shown in Fig. 4. Both profiles create a weak sub-surface sound channel between 0 and 20 m depths and a strong mid-column channel between 30 and 70 m where the sonar and submarine were located. The differences in the profiles were attributed to the significant tidal currents over the LaHave Bank, [7].

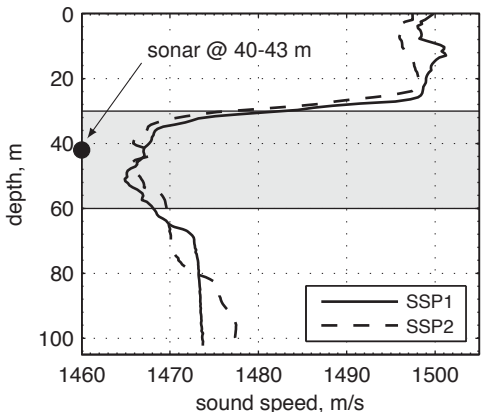

Fig. 4: Measured sound speed profiles. The shaded rectangle is the submarine depth envelope.

Representative sound propagation paths from the sonar for sound speed profile SSP2 are shown in Fig. 5. The submarine dimensions (14 m height and 90 m length) and assumed depth envelope and are included in the figure. Rays launched at angles shallower than ±6.5° were trapped in the sound channel and interacted neither with surface nor bottom. For intermediate launch angles, ±6.5° to ±11.5°, the rays were refracted and reflected from the sea-floor only. Rays with launch angles steeper than ±12° were reflected from the surface and bottom. The ray trace demonstrates that in the trial bottom scattering dominated reverberation.

The temperature and salinity profiles were not measured. Instead, the historical profiles for the LaHave Bank were used in estimation of the Francois-Garrison volume attenuation, [6], at 40 m depth: −3.9 dB/km at 21 kHz and −10.2 dB/km at 39 kHz.

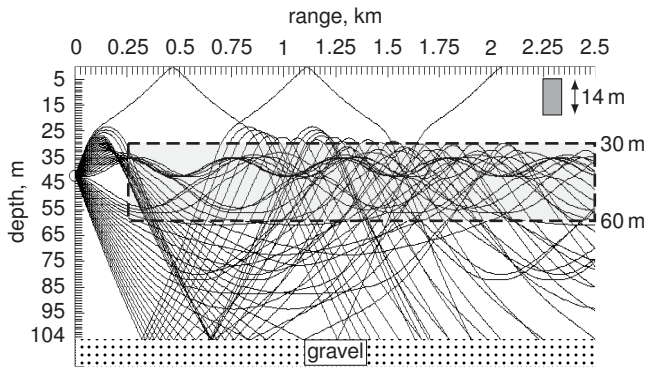

Fig. 5: Representative propagation paths from the sonar at 42 m for sound speed profile SSP2. Ray launch angles are $-12, -11.5, \ldots, 12°$. Shaded rectangles are ▭ submarine dimensions and ⊏ ⊐ submarine depth envelope.

4 Reverberation

For reverberation analysis, 10–15 pings for each frequency and pulse type were selected from the data collected in the target strength trial. These measurements, at 20–24 kHz, 27–29 kHz, and 35–39 kHz, were collected on different bearings as shown in Fig. 2. The reverberation measurements were 2–4 minutes long and ½–1 hour apart. Since the bottom composition and water depth were uniform at the trial site, the reverberation measurements on different bearings could be compared directly.

For estimating of the reverberation from a CW pulse, the received signal was divided into short overlapping segments and the power spectrum of each segment was computed. The length of each segment was equal to the CW pulse length; the range offset between consecutive segments was 5 m. The received echo power was concentrated in the seven frequency bins centered on the pulse center frequency and, at each range, the CW reverberation increment was defined as the total power in these bins.

The reverberation from an LFM ping was evaluated by applying sub-kernel or semi-coherent processing to the received echoes. The received signal was correlated with 400 Hz wide, 32 ms long, 50% overlapped segments of the transmitted pulse replica. The correlation outputs were scaled by the sub-kernel length, converted to power, and averaged. The average power was the FM reverberation time series at the matched filter output.

4.1 CW reverberation

The 28 kHz CW reverberation measurements are presented in Fig. 6 together with the CASS-GRAB predictions for profiles SSP1 and SSP2 and the environment parameters in Section 3. The predictions were for 202 dB re 1 µPa @ 1 m source level and 80 ms pulse length; the measurements were adjusted to the same source level and pulse length. Typically, these adjustments are applied to the model results; however, comparison between measurements at different frequencies (with different source levels and pulse lengths) required adjustment of the measured values to a common source level and pulse length.

For ranges less than 1.8 km, the reverberation predictions agreed with the measurements, except for the sharp peaks

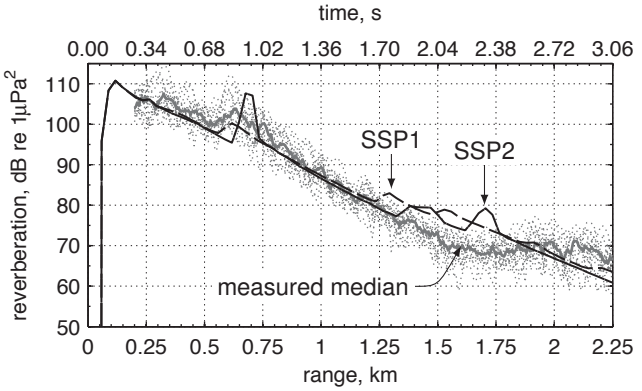

Fig. 6: Measured and modeled 28 kHz reverberation. Dotted lines are individual measurements.

in the SSP2 predictions. The peaks at 0.7 and 1.7 km were caused by the caustics formed by the upward launched rays which interacted with the bottom at these ranges. The broad peak at 1.4 km was caused by the downward launched rays that impacted the bottom at 1.1–1.5 km. The absence of sharps peaks in CASS-GRAB predictions for SSP1, in comparison to SSP2, was due to the small differences between the profiles.

At ranges beyond 1.8 km, where the measured reverberation leveled off, the predictions continued to decrease and underestimated the measurements. At these ranges, the ambient noise was at least 10 dB below the reverberation and did not account for the nearly constant receive levels. Attempts at producing a better fit to the experimental data at the longer ranges by changing the scattering and loss parameters all yielded poorer fits. After these investigations, the long range model-measurement discrepancy was attributed to a propagation effect not included in the propagation model.

The 24, 28, and 39 kHz CW reverberation measurements and CASS-GRAB predictions are compared in Fig. 7. The 39 kHz measurements were terminated early since beyond 1.8 km the received levels were ambient noise dominated; the 24 and 28 kHz measurements were at least 10 dB above the ambient noise levels for all ranges. As before, the predictions were for source level 202 dB re 1 µPa @ 1 m and pulse length 80 ms; all measurements were adjusted to the same source level and pulse length.

The 28 and 39 kHz CW reverberation measurements and predictions agreed up to 1.8 km. The discrepancy between the model and measurements at short ranges was consistent with the expected errors in the APL-UW gravel scattering strength

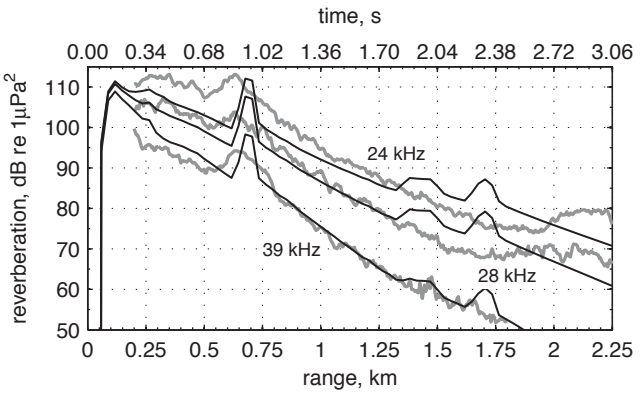

Fig. 7: Measured and modeled reverberation at 20–40 kHz. ——— median measured levels and ——— model output.

(10–15 dB, [6]). The peaks in predictions at 1.5–1.8 km were attributed to the variability in the sound speed profile. At 24 kHz the predicted reverberation underestimated the measurements by 5–10 dB and did not match the observed slope. Beyond 1.8 km none of the predictions captured the leveling off in the measurements.

4.2 CW and FM reverberation

Consistency of the sonar source levels, sensitivities, and beam patterns at adjacent frequencies was verified through comparison of the CW and FM reverberation.

The range resolution of the 60–80 ms long CW pulses was 45–60 m. The FM pulse resolution after 400 Hz sub-kernel processing was 1.9 m. As a result, the FM reverberation levels, at the matched filter output, were 13.8–15.1 dB lower than the CW levels. In cases where FM and CW pulse frequencies did not overlap (20–22 kHz LFM and 24 kHz CW, or 35–37 kHz LFM and 39 kHz CW), additional adjustments to FM levels were necessary to compensate for the frequency dependence in the sonar beam patterns, and volume attenuation.

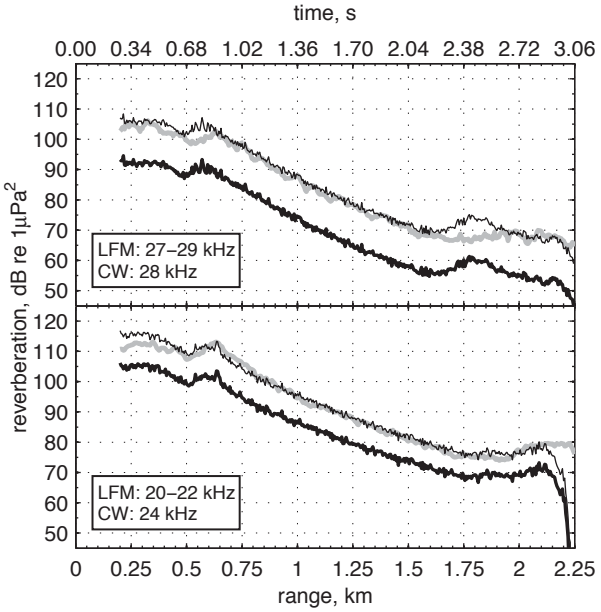

Fig. 8: CW and FM reverberation comparison. ——— CW reverberation measurements. ——— FM reverberation at matched filter output. ——— adjusted FM reverberation.

The CW and FM reverberation is compared in Fig. 8. All levels were adjusted to the same source level 202 dB re 1 µPa @ 1 m. After correction for the pulse type, beam patterns, and volume attenuation differences, the CW and FM reverberation matched indicating consistency of the assumed sonar parameters with the reverberation measurements. The difference in the 28 kHz CW and 27–29 kHz LFM reverberation at 1.8 km was attributed to the variability in the environment since these measurements were taken 30 minutes apart and on different bearings (see Fig. 2) .

5 Propagation Loss

Throughout the trial, the Seahorse sonar was in the mid-column channel at 40–43 m depth. Although the submarine depth was not recorded, it was assumed, in accordance with the trial plan, to be in the mid-column channel: minimum sail depth 30 m depth and maximum keel depth 60 m.

In the submarine depth envelope, the ray density varied with depth and range (see Fig. 5) and the propagation loss was expected to depend on the receiver depth. The dependence is illustrated in Fig. 9 that shows one-way, 24 kHz propagation loss between the sonar and receivers positioned at 1 m depth increments from 30 to 60 m. The loss predictions were computed for the environmental parameters in Section 3. At ranges less than 0.9 km, the modeled propagation loss exhibited large variability with depth. Beyond 0.9 km, this spread in the modeled loss decreased to 5–10 dB.

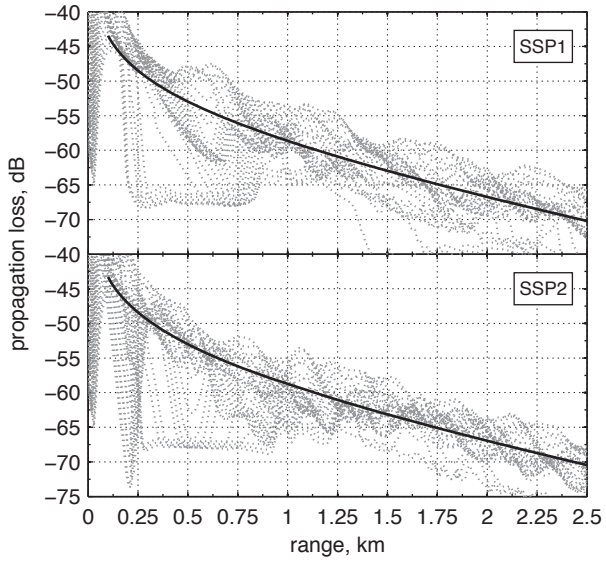

Fig. 9: Modeled propagation loss for 42 m deep source and profiles SSP1 and SSP2. ····· predicted loss for receivers at $30, 31, \ldots, 60$ m depths. ——— least-squares fit to the median of the predicted losses.

Since target highlights at different depths contribute to an echo from the submarine, a depth averaged propagation loss was assumed appropriate for target strength estimation. In a sound propagation channel, where the sonar and the target were located, the average propagation loss is similar to a power law spreading, [8],

$$I(r) = I(1\,\mathrm{m}) \left(\frac{1\,\mathrm{m}}{R_0}\right)^2 \left(\frac{R_0}{r}\right)^a 10^{0.1\alpha r_{\mathrm{km}}} \qquad (2)$$

where $I(1\,\mathrm{m})$ is the sound intensity at 1 m from the source and R_0 is the range where the spherical spreading changes to spreading in the channel. The term $10^{\{\ldots\}}$ is the loss due to volume absorption: α is the volume attenuation coefficient and r_{km} is the range in kilometers.

The propagation loss parameters were estimated via a least-squares fit of the curve

$$PL(r) = A \log_{10}\left(\frac{r}{1\,\mathrm{m}}\right) + B + \alpha \cdot r_{\mathrm{km}} \qquad (3)$$

to the median of the modeled propagation loss over the receivers depths 30–60 m. The fit parameter $A = -10a$ is the spreading loss coefficient, [2]; it is -10 for cylindrical spreading and -20 for spherical spreading. The other fit parameter, B, determines the range for transition between

	A	B	R_0(m)
SSP1	−11.5	−19.3	190
SSP2	−11.3	−20.4	220
mean	−11.4	−19.9	205

Table 1: Least-squares fit parameters for the average propagation loss in the mid-column sound channel.

spherical spreading and channel spreading; the transition range is $R_0 = 10^{-0.1B/(2-a)}$ meters. The average propagation losses for 24 kHz and profiles SSP1 and SSP2 are shown in Fig. 9; Table 1 lists parameters A, B, and transition range R_0.

Although the differences in the propagation losses for sound speed profiles SSP1 and SSP2 could be substantial for specific source and receiver depths, the average losses for the two profiles were nearly identical and similar to cylindrical spreading. In addition, the fit parameters changed little when higher loss surface or bottom reflection loss models were used suggesting that the shallow launch angles dominated the average propagation loss. Since the average propagation loss did not depend strongly on the environment, the mean fit parameters were assumed sufficient for target strength estimation.

Peak submarine target strengths at bow aspect, computed using the average propagation loss are shown in Fig. 10. For CW echoes with low range resolution, the peak intensity corresponded to the echo from the entire hull. For FM pulses with fine resolution, the peak intensity corresponded to the echo from the sail. The target strength estimates were range independent, apart from the statistical variability, suggesting that the propagation loss model was consistent with the propagation conditions during the trial.

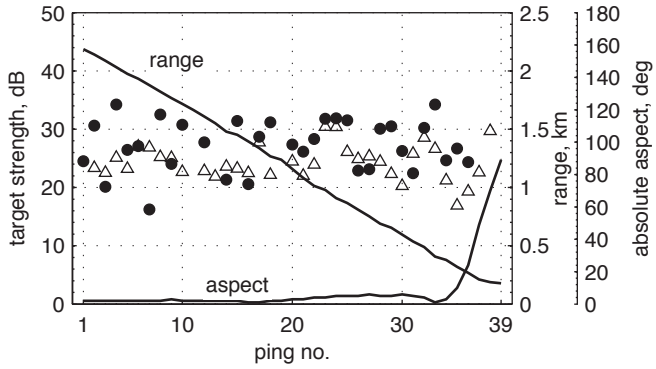

Fig. 10: Submarine peak target strength for bow aspect: ● CW and ▲ FM.

6 Conclusion

The assumed environment and sonar parameters for propagation modeling were verified through comparison of the CW and FM reverberation predictions and measurements. The CW and FM reverberation measurements matched after the FM measurements were adjusted for different pulse range resolutions and frequency dependence in volume attenuation, scattering strength, and beam patterns. For ranges less than 1.8 km, the agreement between the measured and modeled CW reverberation was satisfactory for 28 and 39 kHz; the observed differences were consistent with sound speed variability and expected errors in bottom scattering strength. At 24 kHz, the predictions did not replicate the slope in the measurements and under-predicted the data by 5–10 dB. Beyond 1.8 km, the measured reverberation at all frequencies leveled off whereas the predictions decreased resulting in 5–10 dB under-prediction. The discrepancy was attributed to a propagation effect not captured in the propagation model. More frequent sampling of the environmental parameters is necessary to investigate this hypothesis.

For target strength estimation, an average propagation loss was evaluated by fitting a power law dependence to the predicted losses in the assumed submarine depth envelope. The predictions relied on the environment and sonar characteristics verified in reverberation modeling. The sonar and the submarine were located in a sound channel and the average losses were similar to cylindrical spreading. The estimated propagation loss yielded range independent submarine target strength suggesting that the propagation loss model was consistent with the propagation conditions during the trial.

Acknowledgments

The authors would like to thank Dr. D. Ellis and Dr. S. Pecknold, DRDC Atlantic, for their guidance in reverberation modeling.

References

[1] P. Hines and D. Ellis. High-Frequency Reverberation In Shallow Water. *IEEE J. Ocean. Eng.*, 22(2):292–298, April 1997.

[2] P. Hines, A. Collier, and J. Theriault. Two-Way Time Spreading And Path Loss In Shallow Water At 20–40 kHz. *IEEE J. Ocean. Eng.*, 22(2):299–308, April 1997.

[3] H. Weinberg. *CASS V4.0 User's Manual*. Anteon International Corporation, April 2004.

[4] P. Hines, J. Hutton, and A. Collier. Free-Floating, Steerable, HF Sonar for Environmental Measurements. *Proceedings of IEEE OCEANS'93*, pages II/65–II/70, 1993.

[5] G. Gilbert, D. Horton, and P. Campbell. Seabed Mapping For DREA Experimental Sites. Contractor Report DREA/CR96/404, DREA, February 1996.

[6] Applied Physics Laboratory University of Washington. APL-UW High-Frequency Ocean Environmental Acoustic Models Handbook. Technical Report APL-UW TR 9407, Applied Physics Laboratory Univiersity of Washington, Seattle, Washington, October 1994.

[7] J. Osler. A Geo-Acoustic And Oceanographic Description of Several Shallow Water Exerimental Sites On the Scotian Shelf. Technical Memorandum 94/216, DREA, November 1994.

[8] R. Urick. *Principles of Underwater Sound*. McGraw-Hill, Inc, 2 edition, 1975.